Do Bench-Tests Keep Up With Current Technology in EMI Receivers?

Mario Monti
Elettronica Monti
Ponte a Egola, Italy
Email: monti@elettronicamonti.it

Elena Puri
Elettronica Monti
Ponte a Egola, Italy
Email: elena@elettronicamonti.it

Massimo Monti
Elettronica Monti
Ponte a Egola, Italy
Email: massimo@elettronicamonti.it

***Abstract*—Today, instruments can exploit Fast Fourier Transform (FFT) processing to measure electromagnetic interferences (EMIs). The advantages of such an approach are undisputed. EMI receivers benefit from the extremely short measurement time, compared to that obtained with traditional (super-) heterodyne technology, and of the complete digitalisation of the signal processing. However, not all processing techniques that work correctly in other application fields suit well the demanding measurements of EMIs. Unfortunately, current standards do not prescribe specific tests to check the validity of newly introduced techniques. In this paper, we show that techniques, such as multi-resolution analog-to-digital conversion and measurement repetition, do not always bring advantages in the EMI context and cannot be used to compensate deficiencies in the hardware. We validate our argumentations with lab experiments, where we prove our claims with one of the most well-performing FFT-based EMI receivers that is available today on the market.**

***Index Terms*—FFT Receiver, Dynamic Range, Multi-Resolution ADC, Impulse, CISPR 16-1-1**

I. Introduction

EMI receivers are specialised instruments that are specifically designed to measure electromagnetic interference (EMI). Unlike spectrum analysers that visualise and characterise the spectrum of typically *known* signals in the frequency domain, EMI receivers must deal with *unknown* interferences whose amplitude covers a wide dynamic range and whose frequency spectrum spans over a wide band. Further, the interference repetition rate can be as low as a few Hz or can even be non repetitive. In fact, IEC cites in [1], §6.2 disturbances occurring as *single* or multiple events. Similarly, CISPR 16-1-1 prescribes tests on isolated broadband interferences.

Since decades, CISPR 16-1-1 standard defines the requirements for EMI receivers in the civilian contexts, in order to benchmark these instruments in different setups and environments. For example, EMI receivers must use specific detectors (*e.g.*, peak, quasi-peak, average, RMS) and resolution bandwidths (RBW, *e.g.*, 200 Hz, 9 kHz, 120 kHz, 1 MHz), as defined in [2]. To be able to comply with all requirements of CISPR 16-1-1, EMI receivers need to have a high dynamic range. For example, the prescriptions on the pulse response of the QP detector for an isolated impulse (see Tab. 2 in [2]) are particularly challenging.

Traditionally, EMI receivers were (super-) heterodyne receivers that were tuned consecutively over the different frequencies in order to cover the entire band with the requested RBW. Thus, the time required to perform a measurement was strictly related to the measured bandwidth and the desired resolution. For wide spans, the measurement times could be very long. With the advancement in technology, new EMI receivers have been introduced to reduce the measurement time: the so-called Fast Fourier Transform (FFT) EMI receivers (for a brief overview on the evolution of EMI receivers see [3]). In theory, these modern receivers allow measuring the whole band at once; they digitalise the signal, perform the Fourier transform to estimate the signal spectrum, and then apply the desired detection. They offer a high speed, all benefits of a complete digital signal processing and additional alternative facilities such as statistical analyses.

CISPR 16-1-1 standard was originally developed for traditional heterodyne EMI receivers and today, it only partially refers to the new technology. The standard does not prescribe tests specifically thought for FFT receivers and that check the validity of newly-introduced signal processing techniques.

Today, with the complete digitalisation of the signal processing, new methods have been implemented to improve the performance in the measurement of certain types of signals and in certain conditions. A/D approaches, known as scaled or multi-resolution ADCs [4], may be used to increase the range between maximum and minimum signals that a receiver can correctly measure separately. Repeated measurements can reduce uncertainty [5], for example introduced by the processing of the digitalised signal. Multi-sampling techniques [6] help reducing instrument distortions caused by non-linearities in the different components of the receiving path (amplifier, ADC and possibly filters). Subtraction of the receiver noise, which is measured in a first calibration measurement, can reduce the noise floor [7].

Although such processing techniques can be successfully implemented, for example, to improve performances of spectrum analysers, they fall short of improving (or may even worsen) the measurement capabilities of EMI receivers. They cannot be exploited to substitute well-performing hardware. In this paper, we explain our concerns and show that, unfortunately, measurement uncertainties and errors cannot be compensated via the above mentioned processing techniques. Specifically, in Sect. II, we briefly introduce FFT receivers, focussing on the dynamic range necessary for EMI measurements and discussing issues such as the measurement

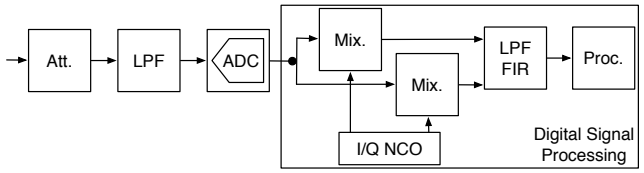

Fig. 1. Simplified block scheme of a Fast Fourier Transform (FFT) EMI receiver, made of attenuator (Att.), low pass filter (LPF), analog-to-digital converter (ADC), complex numerically controlled oscillator (I/Q NCO), mixers (Mix.), digital low pass filter (LPF FIR) and final processing (Proc.)

uncertainty introduced by the modern FFT technology. In Sect. III, we explain two signal processing techniques that are used in some FFT receivers and their drawbacks in EMI measurements. In Sect. IV, we report our measurement results performed with a state-of-the-art FFT receiver that adopts the mentioned processing techniques. In Sect. V, we discuss our experiments and in Sect. VI, we conclude this paper.

II. FFT Receivers

In FFT receivers (see the related basic block scheme in Fig. 1) the whole bandwidth under measurement (limited by a low pass filter, LPF) is given to an ADC, which is placed at the front of the reception path. After digital conversion, time-domain samples are windowed, thus obtaining the needed RBW, and FFT algorithms are used to convert data into the frequency domain. Finally, data is processed to apply the required detection. FFT receivers greatly reduce the time required to perform a measurement since they measure the entire band at once by making first a time-domain acquisition and then the processing in the frequency domain.

There are no intrinsic limitations in applying FFT approaches for measuring EMIs. Instead, there are limitations in implementing FFT receivers due to today's hardware. Differently from common beliefs, these hardware limitations do not come from limited memory or too low sampling rates. Indeed, a system which is specifically designed to process EMI *at real time* does not need to store the signal in a memory (other than mere FFT buffering) and then process it later. Additionally, current A/D technology allow sampling rates of more than 2.5 GS/s that are well capable of satisfying the Nyquist sampling criterion. Instead, the actual bottleneck of the system is insufficient SINAD values of the A/D stage which limit the *dynamic range* of EMI receivers. As a result, to guarantee the correct reception of any type of EMI, the bandwidth that the instrument is able to process in one shot must necessarily be limited. Refer to [8], for a detailed discussion and numerical examples.

A. Dynamic Range

The dynamic range is defined as the linear ratio (or the logarithmic difference) between the maximum and minimum level of signals that a receiver can correctly and *simultaneously* handle. This parameter is also called instantaneous dynamic range [9]. 'Simultaneously' implies that the signals are measured in one shot. The minimum level is the lowest detectable level above the noise. The maximum level is the highest level a receiver can handle without compressing the signal.

As already explained in [10] the noise floor, and thus the minimum level, depends on the type of detector used and on the RBW. Instead, the maximum level depends on the energy that a receiver is able to handle, and is thus dictated by the signal type and amplitude and may depend on the receiver's RBW. The most challenging signals in EMI measurements are pulse signals, where the input energy is spread over the whole input bandwidth [11]. To avoid that a receiver compresses such high-energy signals, the energy must be limited before the signal arrives to the first compression sensitive component. This can be done by reducing the input bandwidth through a filter: the narrower the bandwidth, the lower the energy and thus the higher the maximum measurable level. Obviously, in case of a pulse signal, the maximum measurable level depends on the RBW: the narrower the RBW, the lower the maximum measurable level. In previous publications, see [10] and [8], we clearly showed that the maximum measurable level of a pulse signal compared to a single sinusoidal signal is significantly lower and we proved that, to be able to correctly measure pulse signals, a very high dynamic range is needed.

While in traditional (super-) heterodyne EMI receivers the dynamic range may not represent a critical design aspect, in FFT receivers the dynamic range must be carefully considered. Indeed, traditional EMI receivers perform the measurement by consecutively tuning the receiver over the different frequencies and thus, they can use a narrow preselector to limit the input energy. Instead, in FFT receivers the whole input bandwidth is measured at once. This means that the first components in the receiving path are exposed to a very high energy and may easily overload, hence causing amplitude changes in the reading of input signals.

B. Measurement Uncertainty

Before applying FFT algorithms, a necessary stage in the processing of the signal in FFT receivers is *windowing* [12]. Basically, signal samples are multiplied by the coefficients of a certain window function. This serves to reduce the effect of discontinuities at endpoints of input data. In this process, amplitudes of time samples are smoothly down-scaled the more they are away from the middle of the window. This means that a signal that falls close by the ends of the window is underestimated (erroneous estimation) or even completely missed (erroneous detection) [12].

A commonly used window is the Gaussian window (see the blue curves in Fig. 2). The mathematical definition of a Gaussian window is given by

$$w(n) = e^{-\frac{1}{2}\left[\alpha \frac{n}{N/2}\right]^2} \tag{1}$$

where n is the sample index, N is the number of samples, and α is the parameter that defines the 'width' of the window [12]. The parameter α affects the measurement error due to the weighting of time samples of the signal. Higher α values lead to higher uncertainty. But parameter α also plays a crucial role in the *scalloping* loss, namely the loss in amplitude due

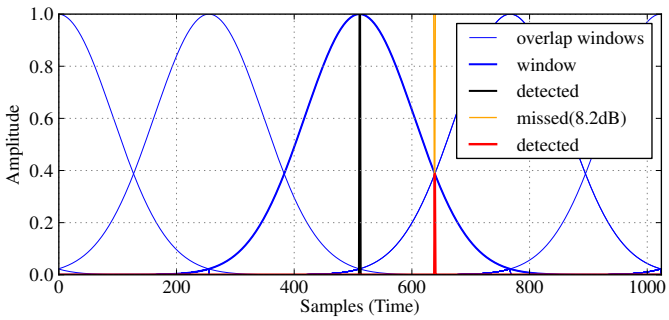

Fig. 2. Overlapped Windowing: Gaussian windows ($\alpha = 5.5$) with an overlap of 75%. This makes the maximum time-domain measurement error 8.2 dB. An impulse (black) that falls in the middle of the window is estimated correctly. An impulse that falls between two consecutive windows is only partially estimated (red); 8.2 dB are lost (orange). Measurement units of both axes are neglected because absolute values are not relevant.

to signal frequency components that fall half way between two bins in the frequency domain [12]. The parameter α is uniquely determined by prescriptions on the scalloping loss as well as on the measurement error in the time domain. Hence, α represents a trade-off to obtain acceptable scalloping losses and time-domain measurement errors. For numerical examples and a more detailed discussion on the measurement uncertainty due to the windowing process, refer to [8].

A common approach to solve the measurement error in the time domain is performing several FFTs over overlapped intervals of samples.[1] Fig. 2 shows the procedure in time domain. The more the overlapping is, the less the measurement error is, but the more FFTs are required to cover a certain number of points. The counterpart of overlapping with high factors, in order to reduce the measurement error, is the high computational load required to perform the many FFTs. In practice, either many parallel hardware modules (FPGAs) must simultaneously compute FFTs over overlapped intervals, or a single switched module must perform consecutive FFTs at a higher speed.

III. Advanced Processing Techniques for FFT Receivers: Advantages and Disadvantages

In this section, we discuss in detail two main techniques that are used to improve performances of FFT receivers: multi-resolution A/D conversion and repeated-measurements for uncertainty reduction.

A. Scaled (Multi-Resolution) ADCs

A/D approaches, known as scaled or multi-resolution ADCs, make larger the range between maximum and minimum signals that a receiver can correctly handle *separately* (signals must be not concurrent). In Fig. 3, we show the basic functioning of scaled or multi-resolution ADCs. For the digitalisation, the signal is split into several channels (*e.g.*, 2 channels in Fig. 3); each channel has its own attenuator (*e.g.*, 0 dB and

[1]Overlapping does not affect the scalloping loss.

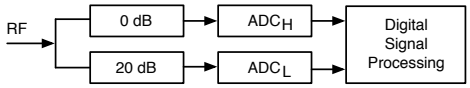

Fig. 3. Scaled or multi-resolution A/D conversion scheme.

20 dB) and own ADC. Each A/D channel covers an interval of the overall amplitude range of the input signal (see [4], [13], [14] for detailed explanations). Our concerns do not relate to possible errors and uncertainties due to unbalanced input channels as for example pointed out in [15]. Rather, we see shortcomings in the concept behind multi-resolution A/D conversion schemes.

In fact, such an A/D approach is equivalent to a classic single ADC preceded by a super fast attenuator with no delay to switch between different attenuation levels. This A/D scheme is able to shift the working point of the receiver but does not increase the (instantaneous) dynamic range. Suppose that two signals of different amplitude form the input to a receiver with multi-resolution ADCs. The presence of the higher-amplitude signal (coexisting with the lower one) makes that mainly the ADC channel covering higher levels works. The ADC channel covering lower levels is blinded (for most of the time). Thus, the lower-amplitude signal is detected wrongly or can even be missed altogether. For detailed numerical examples refer to [8].

B. Repeated Measurements

Statistical approaches in EMI measurements can compensate measurement errors of different nature: measurement uncertainty derived from the time-domain weighting of the signal in the windowing process, harmonic distortion introduced by some components in the receiving path (e.g., ADC, amplifiers, filters), and other sources of errors such as a too high noise floor. For example, instead of performing a single signal acquisition with a subsequent FFT processing using high overlapping factors (e.g., more than 75 %), it is possible to perform several signal acquisitions with subsequent FFT processing using reduced overlapping. Of course, to benefit from this method in terms of hardware resource reduction, the different signal acquisitions and processings are performed sequentially. In this way, the hardware can perform less demanding tasks, *i.e.*, FFTs with lower overlapping factors (e.g. 75 %), in consecutive steps. Similarly, the multi-sampling techniques explained in [6] exploit repeated measurements to reduce/eliminate spurs due to the A/D conversion. By repeating the EMI measurement with different sampling frequency values, spurs appear at different frequencies, while the signal components remain at the same frequencies. The obtained spectra are then minimised and so the EMI's spectrum is derived without (or with reduced) spurs.

Already many publications in the context document the statistical properties of EMIs and give analytical descriptions of FFT receivers. Works such as [16], [17] propose mathematical models of EMIs and discuss statistical properties of different signal processing techniques. In this paper, we simply point

out that there is an indispensable condition for the repeated-measurement approach to work: EMIs must be repetitive.

For example, suppose pulses are detected with a receiver that uses an overlapping as that depicted in Fig. 2. The worst-case scenario is represented by the red impulse of Fig. 2; the impulse falls (in time) exactly between two consecutive windows, and thus is detected with an error of 8.2 dB. If the pulse is repetitive, the more measurements are performed, the more likely the error is reduced. Of course, if the impulse is not repeated, *i.e.*, it is isolated/single, no further measurements are possible. The error cannot be compensated and thus, the receiver is not able to correctly detect the interference.

Generally, statistical approaches in EMI measurements require frequency components and amplitude levels to be stationary so to guarantee that repeated measurements of a certain set of frequencies produce the same results (assuming that the setting of the receiver does not change meanwhile) [6]. While this is true for example for continuous signals and for pulse signals that have a non-zero pulse repetition frequency (PRF), this is not true for an isolated impulse.

IEC includes in [1], §6.2 disturbances occurring as *single* or multiple events. Similarly, CISPR 16-1-1 prescribes tests for EMI receivers on *isolated* broadband interferences. After all, the sole difference between EMI receivers and other types of instruments is the capability to quantify these challenging disturbances.

IV. Lab Experiments

In the following we report the results of various experiments performed using a CISPR 16-1-1 full-compliant Gauss Instruments TDEMI 1G receiver. We chose this instrument as it represents a state-of-the-art receiver which has the unique input bandwidth of 162.5 MHz and which, according to its specifications, exploits the multi-resolution A/D conversion scheme and other advanced processing techniques such as multi-sampling for harmonic distortion reduction. We used the TDEMI 1G receiver in receiver mode, as it guaranteed better performance (not in terms of measurement times) than in spectrogram mode. To cross-check the correctness of the setup and to verify the expected theoretical values, we used a PMM 9010F EMI receiver, which is still based on an FFT signal processing but has a much reduced input bandwidth of 2 MHz.

In the first experiment, we evaluate the difference in EMI measurements in case of (i) a single tone, (ii) two tones both in the band of interest, and (iii) a single tone in the band of interest and one tone out of the band. In the second experiment, we compare the results of the pulse response of the QP detector as described in CISPR 16-1-1 with the results of the same test repeated in the presence of a single tone, out of the band of interest.

A. Experiment 1

Using two different generators (a Rhode & Schwarz SMY Generator and an Agilent 33521A Generator), we generated two continuous-wave sinusoidal signals of different amplitude and frequency. By means of a resistive combiner, we mixed the two signals and produced a single multi-tone interference to be measured with the receiver. To guarantee the absence of any inter-modulation between generators, we attenuated the two signals at the output of the generators by 50 dB and 20 dB, respectively. As a result, considering the further attenuation of 6 dB of the combiner, the total separation between the two generators was 76 dB.

TABLE I
Peak and AVG readings of a single tone signal (125 MHz) for different signal levels with and without a coexisting in-band (110 MHz) or out-of-band (10 MHz) signal

	Signal 1	Signal 2	Sig.1 Reading		Difference	
	Level dBμV	Level dBμV	Peak dBμV	AVG dBμV	Peak dB	AVG dB
Sig.2 inband	40	OFF	40.3	40.2	7.5	0.7
	40	100	47.8	40.9		
	30	OFF	30.3	29.9	15.9	5.8
	30	100	46.2	35.7		
Sig.2 out of band	50	OFF	50.2	50.1	3.14	-0.1
	50	100	53.3	50.0		
	40	OFF	40.2	40.1	7.7	0.6
	40	100	47.9	40.7		
	30	OFF	30.3	30.0	15.7	5.2
	30	100	46.0	35.2		

TABLE II
Peak and AVG noise floor when Signal 2 is off and on

Sig. 2	Peak [dBμV]	AVG [dBμV]
OFF	5	-6
ON	44	34

We performed a band C measurement (30-300 MHz, 120 kHz RBW) using the TDEMI 1G receiver. In Tab. I, we report the readings given by the peak and AVG detectors for a single sinusoidal signal (Signal 1) in presence/absence of the second signal (Signal 2), and related differences. Signal 1 had a frequency of 125 MHz, whereas Signal 2 had a frequency of 110 MHz (inband) for the first part of the experiment and a frequency of 10 MHz (out of band) for the second part of the experiment. The reported levels refer to the levels of the signals after the attenuation. In Tab. II, we also report the noise floor of the peak and AVG detectors when Signal 2 was off and on.

With a single signal, the receiver was capable to correctly measure the signal's amplitude. As soon as we added a further in-band sinusoidal signal (Signal 2), Signal 1 was not measured correctly anymore. The lower the level of Signal 1 was, the bigger the measurement error was. When Signal 2 was out-of-band, the outcome did not improve/change. Thus, we could not measure the single tone signal in band C (*e.g.*, we observed more than 15 dB error) when a single tone with a higher amplitude (*e.g.*, 70 dB higher) was present in band B. The presence of an in-band or out-of-band tone increased the

TABLE III
PEAK AND QP READINGS OF A PULSE SIGNAL FOR DIFFERENT PRFS

PRF Hz	Pk Min dBμV	Pk Max dBμV	QP dBμV	QP Weight dB	Limit dB
100	60.0	60.2	53.1	0 (ref.)	0 (ref.)
20	60.0	60.1	46.9	6.2	6.5±1
10	59.4	59.7	43.3	9.8	10.0±1.5
2	58.0	59.6	31.9	21.2	20.5±2
1	57.2	59.3	31.9	21.2	22.5±2
isol.		**missed altogether**			23.5±2

TABLE IV
PEAK AND QP READINGS OF A PULSE SIGNAL FOR DIFFERENT PRFS IN PRESENCE OF AN OUT-OF-BAND SINGLE TONE SIGNAL

PRF Hz	Pk Min dBμV	Pk Max dBμV	QP dBμV	QP Weight dB	Limit dB
100	54.4	54.7	47.4	0 (ref.)	0 (ref.)
20	53.9	54.4	41.2	6.2	6.5±1
10	53.9	54.4	37.6	9.8	10.0±1.5
2	53.0	54.0	31.6	**15.8**	20.5±2
1	51.4	52.6	31.1	**16.3**	22.5±2
isol.		**missed altogether**			23.5±2

noise floor. As documented in Tab. II, roughly 40 dB higher noise levels were measured when both tones (Signal 1 and Signal 2) were switched on.

B. Experiment 2

We first generated a pulse signal with an area of 89 nVs, a spectral density of 102 dBμV/MHz and a flatness of 1 dB for band B (0.15-30 MHz), using an EM C1611 EMI Receiver Tester. Thus, the theoretically expected peak (using 9 kHz RBW) is $102 - 20\text{Log}(1 \cdot 10^6/9 \cdot 10^3) = 61$ dBμV. In Tab. III, we report peak and QP readings measured at 10 MHz, for different PRFs, using the TDEMI 1G receiver.

Since we observed that the peak reading changed among adjacent frequencies, we provide maximum and minimum peak values in the frequency range $9.5 - 10.5$ MHz. Further, the table reports the relative equivalent level of the pulse (QP Weight, as prescribed in [2], Tab. 2) and also reports the CISPR 16-1-1 QP weight limits for band B for comparison. We made sure the acquisition time of the receiver was greater than the inverse of the PRF. Indeed, we set the acquisition time to 30 s. For the isolated (isol.) or single pulse, we first let the measurement start. After roughly 10 s, we generated the single impulse and finally waited for the measurement.

Repeated pulses gave a correct (well within the CISPR 16-1-1 limits) QP weighting. Instead, the single pulse was missed altogether and thus its QP weighting was not computed. We also noticed an increasing (logarithmic) difference between maximum and minimum peak values with decreasing PRF. Moreover, a difference of up to 3 dB was observed in the peak readings for the different PRFs.

In the second part of the experiment, we added an out-of-band continuous-wave sinusoidal signal of 109 dBμV and 32 MHz (generated using a Rhode & Schwarz SMY Generator) to the pulse signal described above. We mixed the two signals by means of a resistive combiner with 6 dB attenuation. Thus, the expected peak measurement of the pulse signal (using 9 kHz RBW) was $61 - 6 = 55$ dBμV. We repeated the measurements of the pulse signal for different PRFs as in the first part of the experiment, see Tab. IV for the results.

The isolated pulse was again missed altogether and repeated pulses with low rates, *i.e.*, 2 and 1 Hz, could not be measured correctly with the QP detector; there was a 4.7 dB and 6.2 dB deviation, respectively, from CISPR 16-1-1 requirements.

We performed the same tests also in band C. The out-of-band signal (29 MHz) had an amplitude of 100 dBμV. We generated the impulse with an Electro-Metrics CIG 25 Impulse Generator, having a spectral density of 84 dBμV/MHz and a flatness of 2 dB within 1 GHz. The receiver's QP weightings deviated from CISPR 16-1-1 requirements for PRFs below 20 Hz (results not shown for space limitations).

V. DISCUSSION

In the first experiment, measurements of the level of a single frequency component were affected by the presence of signals at other frequencies, even out of the band of interest. We believe that the multi-resolution A/D conversion scheme makes that, when both signals are present, mainly the ADC channel covering higher levels works. The ADC channel covering lower levels is mostly blinded by the high-amplitude signal in both cases, when the signal is in-band as well as when it is out-of-band. As mentioned in Sect. III, having multi-resolution ADCs merely shifts the working point of the receiver but does not increase the instantaneous dynamic range. Our beliefs are confirmed by the increase in the noise floor documented in Tab. II. Since the ADC channel covering higher levels raises the noise floor close to, or even above, Signal 1's level, its level is detected wrongly.

In the second experiment, similarly to experiment 1, the presence of an out-of-band sinusoidal signal resulted in a wrong QP weighting of the pulse signal for low PRFs (2 and 1 Hz). We remark that, in these broadband signal tests, the amplitude of the sinusoidal signal was much lower compared to the broadband pulse signal level. Thus, the voltage seen by the receiver did not change (<0.15 dB difference). Given the generator's spectral density, if we assume a limited bandwidth of 162.5 MHz (best-case scenario, provided a brick-wall preselection equivalent to the declared measurement bandwidth), we obtain a broadband pulse signal level of $20\text{Log}(162.5 \cdot 10^6/1 \cdot 10^6) + 102 \approx 146$ dBμV. Therefore, if we sum up the linear amplitude of the two signals, $20\text{Log}\,(10\hat{}(146/20) + 10\hat{}109/20)) = 146.122$ dBμV, and compare it with the level of the sole impulse, 146 dBμV, we get a negligible difference of 0.122 dB. Thus, any saturation that may justify the measurement errors was averted. In any case, we would expect that a C-band sinusoidal signal would not influence at all pulse measurements in band B.

The difference in QP weightings between the two pulse tests (with and without the out-of-band tone) can be justified by an insufficient instantaneous dynamic range. The wrong QP weighting may be derived from a too high noise floor. As

validated by the noise measurements reported in Tab. II, an out-of-band tone changed the noise floor level of the tested receiver, and consequently changed the detector response.

In [8], we suggested the use of preselection to improve the dynamic range of a receiver in case of broadband EMIs. In experiment 2, preselection would definitely have cut out the out-of-band signal. Preselection would also have helped in case the concurring sinusoidal signal was in band. Indeed, a preselector would have sufficed to limit the input bandwidth of the impulse, in this way, making the dynamic range high enough to correctly weight the impulse at low PRFs. In experiment 1, again, preselection would have cut out the out-of-band sinusoidal signal. On the contrary, preselection would not have helped in the case when both sinusoidal signals were in band. Indeed, in case of (in-band) narrow-band signals, the energy is concentrated in a few frequency components and it is thus not affected by preselection.

Peak readings were affected by an increasing uncertainty for decreasing PRFs (see Tab. III). For a PRF of 1 Hz, the difference between maximum and minimum peak readings in adjacent frequencies was of more than 2 dB. Additionally, the difference in peak readings for different PRFs was of up to 3 dB. This increasing uncertainty might be due to an insufficient measurement repetition. While high PRF values make possible to capture the pulse signal several times, low PRFs do not allow a sufficient number of measurements.

Unfortunately, CISPR 16-1-1 requirements include only a single *absolute* calibration measurement that controls a correct relationship between peak and QP readings (see Tab. 7 in [2]). All other requirements are based on this reference measurement and are thus only *relative* measurements (*e.g.*, the relative QP pulse response in [2], Tab. 2). Hence, the receiver is calibrated to measure peak values under certain conditions but not for other conditions where only relative QP values are observed. Thus, it can happen (as in experiment 2, Tab. III) that the relative values as prescribed in [2] are within the limits, while the absolute reading is underestimated.

We highlight that the tests we performed with concurrent signals (whose results are shown in Tabs. I and IV) are not prescribed by current standards. However, we believe that similar tests may represent the mean to verify the correct reception of all types of EMIs and in all conditions.

VI. Conclusion

We strongly believe that FFT receivers represent the present and the future of EMI measurements. The parallel measurements of an enormous number of frequency components can only benefit EMI measurements. There are no intrinsic drawbacks in FFT approaches for EMI reception. There are, instead, intrinsic limitations derived from the nowadays-available hardware (mainly analog to digital conversion). If the hardware in the reception path of FFT receivers is not designed taking in consideration the challenging objective of estimating correctly any kind of interference, there are no (post-)processing techniques that can compensate the derived measurement errors. The use of general-purpose hardware as well as an excessive input bandwidth even with state-of-the-art technology can lead to insufficient performances, which cannot guarantee the correct measurement of EMIs. Standards in the context have been thought to challenge a different type of receivers, and in a time when some processing techniques were not yet realisable for EMI reception. We believe that current standards, which have started including the concept of FFT receivers, still miss some specific tests to estimate the actual quality of the instruments for EMI measurements.

References

[1] "Electromagnetic compatibility (EMC) - part 2-5: Environment - description and classification of electromagnetic environments," TR 61000-2-5 Ed 3.0, International Electrotechnical Commission, Jan 2017.

[2] "Specification for radio disturbance and immunity measuring apparatus and methods - part 1-1: Radio disturbance and immunity measuring apparatus - measuring apparatus," CISPR 16-1-1 Ed. 3.0, International Electrotechnical Commission, Jan 2010.

[3] M. Rahim, "Evolution and trends of EMI receiver," in *IEEE Intl' RF and Microwave Conference (RFM)*, Dec 2013, pp. 362–367.

[4] S. Braun and P. Russer, "A low-noise multiresolution high-dynamic ultra-broad-band time-domain EMI measurement system," *IEEE Trans. on Microwave Theory and Techniques*, vol. 53, no. 11, pp. 3354–3363, 2005.

[5] C. Keller and K. Feser, "Fast emission measurement in time domain," *IEEE Trans. on Electromagnetic Compatibility*, vol. 49, no. 4, pp. 816–824, 2007.

[6] S. Braun and P. Russer, "Measurements of spurious emission with a time-domain EMI measurement system using multi-sampling techniques," in *IEEE Intl' Symp. on Electromagnetic Compatibility (EMC)*, 2006, pp. 792–795.

[7] A. Technologies, "Using noise floor extension in the PXA signal analyzer," Application Notes, Feb 2010.

[8] M. Monti, E. Puri, and M. Monti, "Hidden aspects in CISPR 16-1-1 full compliant fast fourier transform EMI receivers," in *Intl' Symp. on Electromagnetic Compatibility - EMC EUROPE*, Sep 2016, pp. 34–39.

[9] J. Tsui, *Digital Techniques for Wideband Receivers*. Massachusetts: Artech House Publishers, 2nd ed., 2001.

[10] M. Monti, E. Puri, and M. Monti, "Pitfalls in measuring discontinuous disturbances with latest click analysers," in *IEEE Intl' Symp. on Electromagnetic Compatibility (EMC)*, Jul 2016, pp. 1–6.

[11] D. Schwarzbeck, "The EMI-receiver according to CISPR 16-1-1," Application Notes, www.schwarzbeck.de/appnotes/EMIRcvrCISPR16.pdf, Retr. on Jan 2016.

[12] J. F. Harris, "On the use of windows for harmonic analysis with the discrete Fourier transform," *In Proc. of IEEE*, vol. 66, no. 1, pp. 51–83, 1978.

[13] S. Braun and P. Russer, "The dynamic range of a time-domain EMI measurement system using several parallel analog to digital converters," in *IEEE Intl' Symp. on Electromagnetic Compatibility (EMC)*, Feb 2005, pp. 203–208.

[14] S. Braun, S. Iliev, M. Al-Qedra, and P. Russer, "A real-time multiresolution time-domain EMI measurement system based on ultra-fast high resolution analog-to-digital converters," in *Intl' Conf. on Microwaves, Radar & Wireless Communications (MIKON)*, 2006, pp. 1–4.

[15] M. Kamensky and K. Kovac, "Suitability of pulse error models for time-domain spectrum measurements," *Procedia Engineering*, vol. 69, pp. 415–422, 2014.

[16] M. Azprua, M. Pous, and F. Silva, "On the statistical properties of the peak detection for time-domain EMI measurements," *IEEE Trans. on Electromagnetic Compatibility*, vol. 59, no. 6, pp. 1374–1381, 2015.

[17] ——, "Decomposition of electromagnetic interferences in the time-domain," *IEEE Trans. on Electromagnetic Compatibility*, vol. 58, no. 2, pp. 385–392, 2016.